# The effect of surface tension on the shape of a Hele–Shaw cell bubble

Saleh Tanveer

Citation: Physics of Fluids (1958-1988) **29**, 3537 (1986); doi: 10.1063/1.865831
View online: http://dx.doi.org/10.1063/1.865831
View Table of Contents: http://scitation.aip.org/content/aip/journal/pof1/29/11?ver=pdfcov
Published by the AIP Publishing



# The effect of surface tension on the shape of a Hele–Shaw cell bubble

Saleh Tanveer
*Mathematics Department, Virginia Polytechnic Institute and State University, Blacksburg, Virginia 24061*

(Received 7 April 1986; accepted 30 June 1986)

Numerical and asymptotic solutions are found for the steady motion of a symmetrical bubble through a parallel-sided channel in a Hele–Shaw cell containing a viscous liquid. The degeneracy of the Taylor–Saffman zero surface-tension solution is shown to be removed by the effect of surface tension. An apparent contradiction between numerics and perturbation arises here as it does for the finger. This contradiction is resolved analytically for small bubbles and is shown to be the result of exponentially small terms. Numerical results suggest that this is true for bubbles of arbitrary size. The limit of infinite surface tension is also analyzed.

## I. INTRODUCTION

The problem of viscous flows in a Hele–Shaw cell has received a lot of attention in recent literature. Most of the work, however, has been confined to the study of fingers. The analogous problem of the motion of a finite sized bubble has received scant attention even though such bubbles have been observed in the experiments of Saffman and Taylor[1] and more recently by Maxworthy.[2] Taylor and Saffman[3] consider the motion of a finite sized bubble moving steadily through a parallel-sided channel in a Hele–Shaw cell containing another viscous fluid. Neglecting the surface tension and density of the fluid in the bubble, they obtain a two-parameter family of exact solutions. For fixed width of the cell and velocity of the viscous fluid at infinity, the bubble area and speed can be taken as these two parameters. For a given area of the bubble, they find solutions for arbitrary bubble speeds over some range, with the speed determining the shape of the bubble. A similar degeneracy is found in the zero surface-tension solution for a steadily translating finger in a Hele–Shaw cell, first noted by Saffman and Taylor.[1] The finger width remains arbitrary over some continuous range. McLean and Saffman[4] include the effect of surface tension in their numerical calculations of a steady finger and find that solutions exist only for some isolated values of finger width for a given surface tension. Romero[5] and Vanden-Broeck[6] find other isolated values of finger width for which solutions exist. However, as surface tension tends to zero, all these solutions tend to the Saffman–Taylor solution with finger width equaling one-half the channel width. In that sense, the degeneracy of the Saffman–Taylor finger solutions is removed by surface tension. However, McLean and Saffman note that for small surface tension, apparently consistent perturbation solutions can be constructed around the Saffman–Taylor exact solutions for any value of the finger width. This contradicts numerical evidence which is overwhelming in view of the careful work of multiple investigators. We recalculated the finger solutions using a variation of the method used here and our results confirm the findings of the previous investigators. At about the same time this paper was first submitted, we became aware of the analytical work of Shraiman,[7] Combescot *et al.*,[8] and Hong and Langer[9] which suggest that there are exponentially small terms in surface tension which are not accounted for in the perturbation analysis of McLean and Saffman. These violate boundary conditions unless the finger width is constrained to a discrete set of values depending on surface tension. Here, we will present evidence to show that a similar situation arises for the case of a finite bubble.

The purpose of this paper is to consider the effect of surface tension on the shape of a finite bubble in a Hele–Shaw cell. Our numerical results and analytical arguments suggest that the degeneracy of Taylor–Saffman solutions is removed by the introduction of surface tension, i.e., for specified bubble area and surface tension, there are only isolated values of bubble speed for which a solution exists. However, as for the finger, an apparently consistent perturbation solution can be found for small surface tension for any bubble area and speed over a range, suggesting that the surface tension does not remove the degeneracy of the Taylor–Saffman bubble solutions. Thus a contradiction between numerics and perturbation arises here as it did in the McLean–Saffman analysis of a finger. In this paper, we present strong evidence to show that in general the formal perturbation series in powers of surface tension parameter does not correspond to an actual solution because there are terms of exponential order which are singular in the flow domain and do not satisfy boundary conditions. The condition for the absence of such singularity determines the bubble speed for specified area and surface tension parameters. This result is important because there is no indication from the analysis of a finite number of perturbation terms that the function it corresponds to is singular anywhere in the flow domain. For the case of a small bubble with the surface tension parameter of order 1, an explicit relation between bubble velocity, size, and surface tension is found in a perturbation series involving the bubble size parameter.

For the case when surface tension is small, but the bubble not necessarily so, we present a modified perturbation procedure for the calculation of flow to the leading order in surface tension. The perturbation equation includes the highest derivative terms of the unknown function even though it is multiplied by a small surface tension parameter. The formal perturbation procedure ignores these terms since

 0031-9171/86/113537-12$01.90  

these are expected to be higher order. This is expected to be uniformly true since the boundary conditions appear to be automatically satisfied by the solution to the equation not involving derivatives. However, numerical solution of the modified perturbation equation could only be found when the bubble speed is treated as an unknown for given bubble area and surface tension parameters. This supports our contention that there are exponential order terms in the solution which are responsible for the constraints between surface tension, bubble speed, and area. The relation between these three quantities arising out of the modified leading order perturbation calculations is in agreement to first order in surface tension with the numerically determined constraint relation for the full problem.

The numerically determined solutions are, however, nonunique and it is found that there are more than one value of bubble speed possible for a given bubble area and surface tension. We introduce a procedure to systematically find other isolated branches of bubble solutions. This procedure was applied to relatively small bubbles and we find two possible solutions for given bubble area and surface tension over some range. One branch always appears to correspond to a bubble with positive curvature and its front half, in the limit of large area, tends to the McLean–Saffman finger. We call this branch the main branch. The bubbles corresponding to the second branch (called the extraordinary branch) has the unusual feature of negative curvature over parts of the bubble contour for some range of surface tension and bubble area. This branch appears to exist over a very limited range in the parameter space. It does not appear that this branch of solutions exists when the size parameter is too large. The possibility is open for the existence of other branches of solutions which in the limit of a large area correspond to the Romero–Vanden-Broeck branches of finger solutions. However, we were unable to find such solutions by a continuation procedure from solutions with small bubble area.

We also analyzed the bubble shapes in the limit of infinite surface tension. Three possibilities are noted: In the first case, when the limiting bubble is assumed to have positive curvature and the bubble is too large to be fitted into the Hele–Shaw cell as a circle, there are no solutions. In the second case, when the limiting bubble has positive curvature but is small enough to be fitted into the cell as a circle, the circle is the only possible shape. The third case is when the bubble has negative curvature on parts of its contour. We were unable to get a definite conclusion for such a case. The possibility is open for negative curvature on a part of the boundary adjacent to the front stagnation point of a bubble that elongates indefinitely in the direction of the oncoming flow as surface tension is increased. The rate at which the length of such a bubble (if it exists) increases with surface tension must be at least as fast as a linear growth.

## II. MATHEMATICAL FORMULATION

We consider a finite sized bubble steadily translating with velocity $U$ in a parallel sided Hele–Shaw cell of width $2a$ and gap $b$ between the plates containing a viscous fluid which moves with velocity $V$ far upstream and downstream (Fig. 1). We assume that the bubble leaves no viscous fluid

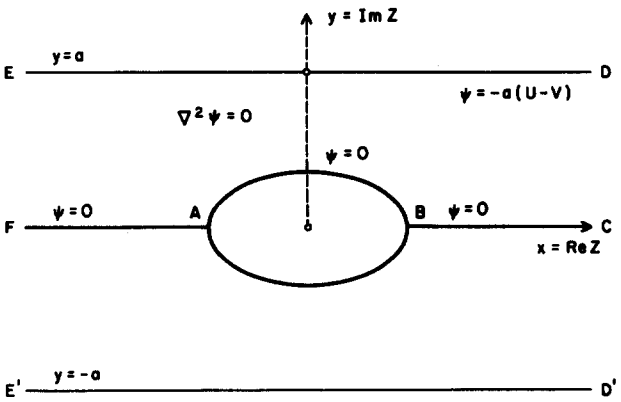


FIG. 1. The flow region in the $z$ plane (physical plane) in the bubble frame.

in the region between the gaps as it advances and that there is no variation in transverse (across the gap) curvature. We restrict ourselves to bubbles which are symmetric about the centerline ($x$ axis) of the channel. We also assume that the bubble surface has no corners of cusps. As in Taylor and Saffman, we assume that the viscosity of the fluid inside the bubble is negligible and that the pressure gradients due to gravity may be ignored.

For a small plate gap, i.e., $b/a \ll 1$, the mean flow across the stratum of the viscous fluid through which the bubble is moving is described by a harmonic potential $\phi(x,y)$ where velocity $(u,v)$ is given by

$$(u,v) = \nabla\phi = (-b^2/12\mu)\nabla p\,, \tag{1}$$

where $p$ is the mean pressure across the stratum and $\mu$ is the viscosity of the fluid surrounding the bubble. We introduce the stream function $\psi(x,y)$ that is the harmonic conjugate of $\phi$. The boundary conditions for the flow are

$$\psi = \pm aV\,, \tag{2}$$

on $y = \pm a$ and as $x \to \pm\infty$,

$$\psi \sim Vy\,. \tag{3}$$

Since the bubble translates with velocity $U$ in the $x$ direction, it follows that on the bubble

$$\psi = Uy\,. \tag{4}$$

The dynamic condition of balance of forces on the bubble boundary implies

$$\phi(x,y) = (b^2T/12\mu)(1/R) + \phi_0\,, \tag{5}$$

where $T$ is the surface tension, $R$ is the radius of curvature of the finger in the $x$-$y$ plane, and $\phi_0$ is a constant independent of $x$, $y$. If we switch to a frame moving with the bubble by introducing transformed variables,

$$\hat{x} = x - Ut, \quad \hat{y} = y\,, \tag{6}$$

$$\hat{\phi} = \phi - Ux, \quad \hat{\psi} = \psi - Uy\,, \tag{7}$$

then $\hat{\phi}$ and $\hat{\psi}$ are harmonic functions of $\hat{x}$ and $\hat{y}$ and

$$\hat{\psi} = \mp a(U - V)\,, \tag{8}$$

on $\hat{y} = \pm a$. As $\hat{x} \to \pm\infty$,

$$\hat{\psi} \sim -(U - V)\hat{y} \tag{9}$$

and on the bubble boundary, the two boundary conditions are

$$\hat{\psi} = 0\,, \tag{10}$$

$$\hat{\phi} + U\hat{x} = (b^2 T/12\mu)(1/R) + \text{const.} \tag{11}$$

From this point onward, we will drop the caret notation with the understanding that all our variables are in the frame where the bubble is stationary. Further, it is clear that we can nondimensionalize all our dimensional variables by using combinations of $a$ and $V$. This is equivalent to setting $V$ and $a$ to unity in all our equations with the understanding that all our variables are now nondimensionalized. We will henceforth refer to these nondimensional variables.

We introduce the complex velocity potential $W = \phi + i\psi$, which is an analytic function of $z = x + iy$. From flow symmetry about the centerline of the channel, it follows that the flow field exterior of the bubble for $y > 0$ corresponds to an infinite strip in the $W$ plane of width $(U-1)$ as in Fig. 2. Consider the conformal mapping of the flow field exterior of the bubble for $y > 0$ into the interior of the unit semicircle in the $\zeta$ plane (Fig. 3) such that the rear and front stagnation points $A$ and $B$ correspond to $\zeta = \pm 1$, and $z = \pm\infty$ correspond to $\zeta = \pm\alpha$, where $0 < \alpha < 1$. Then the upper half of the bubble contour corresponds to the arc of the semicircle. It follows after a sequence of transformations, that with certain choices of origin for $W$ and branch for logarithm,

$$W = -\frac{(U-1)}{\pi}\log\left(\frac{(\zeta-\alpha)(1-\alpha\zeta)}{(\zeta+\alpha)(1+\alpha\zeta)}\right), \tag{12}$$

where $\alpha$ is a parameter related to the size of the bubble.

We define an analytic function $f(\zeta)$ by the relation,

$$z = \frac{1}{\pi}\log\left(\frac{\zeta-\alpha}{\zeta+\alpha}\right) + \frac{1}{\pi}\left(\frac{2}{U}-1\right)\log\left(\frac{1+\zeta\alpha}{1-\zeta\alpha}\right) + (2\alpha/\pi U)\, f(\zeta)\,. \tag{13}$$

From the known properties of the conformal map $z(\zeta)$ on the straight boundaries and in the neighborhood of $\zeta = \pm\alpha$, it follows that $f$ cannot have any singularities on the real $\zeta$ diameter of the unit semicircle. Further, for bubbles with continuous boundaries, it follows from the properties of the conformal map $z(\zeta)$, that $f$ must be continuous on the arc of the $\zeta$ semicircle. Also, from the known values attained by $\mathrm{Im}(z)$ on different parts of the real diameter of

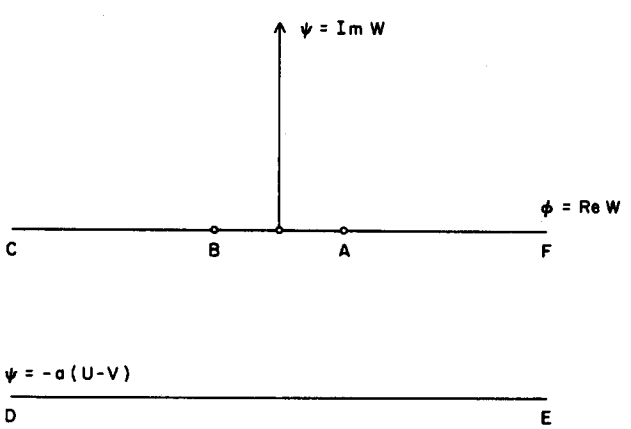


FIG. 2. The flow region in the $\zeta$ plane.

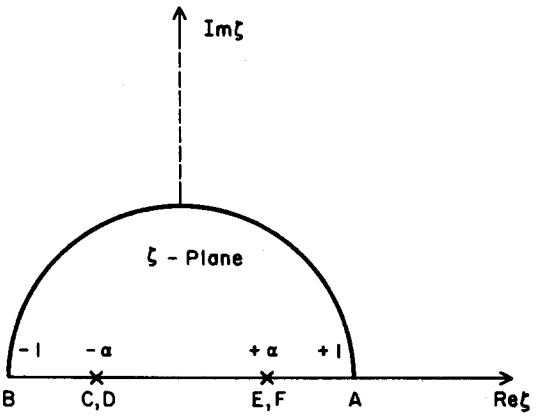


FIG. 3. The flow region in the $W$ plane.

the $\zeta$ semicircle, it follows from (13) after appropriate choice of branches that on $-1 < \zeta < 1$,

$$\mathrm{Im} f = 0\,. \tag{14}$$

From Schwarz's reflection principle it follows that $f$ is analytic on the entire unit $\zeta$ circle and has a convergent power series representation, at least for $|\zeta| \leqslant 1$. From (12) and (13), we find that

$$\frac{dz}{d\zeta} = \frac{2\alpha}{\pi U}\left[f'(\zeta) + h(\zeta)\right], \tag{15}$$

where

$$h(\zeta) = \frac{U(1+\alpha^2)(1-\zeta^2) - 2(\alpha^2-\zeta^2)}{(\zeta^2-\alpha^2)(1-\alpha^2\zeta^2)}\,. \tag{16}$$

Now, $1/R = d\theta/ds$, where $\theta = \mathrm{Arg}(dz)$ and $s$ is the arc-length along the bubble measured from the front stagnation point $B$. It follows that on $\zeta = e^{iv}$ for $0 \leqslant v \leqslant \pi$,

$$\frac{1}{R} = -\frac{\pi U}{2\alpha}\left(\frac{1 + \mathrm{Re}[\zeta(f''+h')/(f'+h)]}{|f'+h|}\right). \tag{17}$$

From (11), (12), (13), and (17) it follows that on $\zeta = e^{iv}$ for $0 \leqslant v \leqslant \pi$,

$$\mathrm{Re} f = -\epsilon\left(\frac{1 + \mathrm{Re}[\zeta(f''+h')/(f'+h)]}{|f'+h|}\right), \tag{18}$$

where $\epsilon = (\pi^2 U/4\alpha^2) b^2 T/12\mu$ and any constant that would otherwise appear on the right-hand side of (18) is absorbed in $f$. (This corresponds to a choice of origin for $x$.) In Eqs. (16) and (18), $U$, $\alpha$, and $\epsilon$ appear as three parameters and it would appear that $f$ is completely determined by the boundary conditions (14) and (18) once these parameters are specified over some range. However, this is not the case for nonzero $\epsilon$. As will be seen later, an analytic function $f$ in the unit semicircle whose first two derivatives are continuous on the boundary and satisfies conditions (14) and (18) can only exist if a constraint is satisfied between these three parameters. We will take $\alpha$ and $\epsilon$ as our two independent parameters. Thus $U$ as well as the function $f$ are unknowns to be determined from (14) and (18). A note is in order as far as our choice of independent parameters. From a physical viewpoint, it would seem more logical to choose the bubble area $J$ and $b^2 T/12\mu$ as our independent parameters. However, we found it more convenient for numerical calculations

to choose the parameters the way we did. Since $U$ is found to vary slowly between 1 and 2 in the range of our numerical calculations, we can consider $\epsilon$ as the surface tension parameter for fixed $\alpha$. Thus $\alpha$ can be regarded as the size parameter, though the bubble area depends both on $\alpha$ and $\epsilon$ as will be seen a little later. The dependence of the bubble area on $\epsilon$ is through $U$ and the function $f$. For fixed $\epsilon$, as $\alpha$ is increased form 0 to 1, the bubble area is found to increase monotonically from 0 to infinity.

It may also be noted that there is one more condition on $f$ which appears to be automatically satisfied by every solution $f$ satisfying (14) and (18). From examination of the properties of the conformal map between domains in the $z$ and $\zeta$ planes, as shown in Figs. 1 and 3, it follows that in or on the unit $\zeta$ semicircle, $dz/d\zeta$ must have no zeros and two simple poles at $\zeta = \pm\alpha$. It is clear from (15) and (16) that these conditions are satisfied when $f = 0$ for $0 < \alpha < 1$ and $U > 1$. The same is true when the maximum norm of $f$ is small enough as can be seen by a simple application of Rouche's theorem. From our numerical calculations of $f$ and $U$ for given $\alpha$ and $\epsilon$, it appears that this condition on the poles and zeros just mentioned holds for every solution $f$ satisfying (14) and (18) at least in the range of parameters investigated in the numerical calculations.

Once $f$ and $U$ are determined for given $\alpha$ and $\epsilon$, the mapping function $z(\zeta)$ and therefore the bubble boundary is determined from (13). We now find an expression for the area of the bubble $J$ in terms of $\alpha$, $U$, and $f$. If we consider only the upper half-bubble contour from the front to the rear stagnation point and parametrize it by arclength $s$, then

$$\frac{J}{2} = \int_0^L x \frac{dy}{ds}\, ds ,$$

where $L$ is the arclength of the bubble contour between the two stagnation points. From (11) it follows that

$$\frac{UJ}{2} = -\int_0^L \phi \frac{dy}{ds}\, ds + \frac{b^2 T}{12\mu} \int_0^L \frac{1}{R} \frac{dy}{ds}\, ds . \tag{19}$$

Using $dy/ds = \sin\theta$ and $1/R = d\theta/ds$, the second term in the above equation integrates out to 0. Since the stream function is zero on the bubble it follows from (19) that

$$\frac{UJ}{2} = \mathrm{Im} \int_{\mathbb{C}} W \frac{dz}{d\zeta}\, d\zeta , \tag{20}$$

where $\mathbb{C}$ is the contour along the semicircular arc in the $\zeta$ plane joining 1 and $-1$. Using (12) and (15), we expand $W$ and $dz/d\zeta$ in the neighborhood of $\zeta = \pm\alpha$ and deform the contour in (20) to coincide with the real $\zeta$ axis except for small semicircular detours around $\pm\alpha$. Using standard techniques in contour integration, the integral in (20) is evaluated and we obtain,

$$(U^2 J\pi)/4 = 2(U-1)\log\left[(1+\alpha^2)/(1-\alpha^2)\right] + \alpha(U-1)\left[f(\alpha) - f(-\alpha)\right] . \tag{21}$$

We note that in (21) the area $J$ depends on both the parameters $\alpha$ and $U$ and that the dependence on the function $f$ enters only through the values of $f$ at two points. We will use (21) later on to investigate the infinite surface tension limit for fixed $J$.

When the surface tension parameter $\epsilon = 0$, $f = 0$ identically. This corresponds to the Taylor–Saffman exact solution which exists for two arbitrary parameters $\alpha$ and $U$ in the ranges (0,1) and $(1,\infty)$, respectively. The quantity $U\lambda$ in the notation of Taylor and Saffman equals $4/\pi \arctan(\alpha)$. For given $U$, as $\alpha$ increases from 0 to 1, the bubble increases in area until in the limit it becomes an infinitely elongated bubble, the front half of which approaches the finger solution of Saffman and Taylor. For given $\alpha$, as $U$ increases from 1 to $\infty$, the bubble shape changes from extreme vertical to horizontal elongation which in the two limits correspond to straight line boundaries. The shape of the bubble for zero surface tension has fore and aft symmetry as can be seen from (13). This symmetry is lost when surface tension is introduced except when the bubble is circular. This can be very easily argued. If we assume that a symmetric bubble is possible, then the left- and right-hand sides of (11) will be odd and even functions of $x$ with the appropriate choice of origin for $x$ and $\phi$ and therefore the equality in (11) is not possible unless the bubble is circular. In the next section we find a perturbation solution for small $\epsilon$.

## III. PERTURBATION SOLUTION FOR SMALL SURFACE TENSION

For small $\epsilon$, we seek a perturbation solution of the form

$$f = \sum_{n=1}^{\infty} \epsilon^n f_n , \tag{22}$$

satisfying (14) and (18). The first-order perturbation $f_1$ satisfies

$$\mathrm{Re}\, f_1 = -\{1 + \mathrm{Re}\, \zeta(h'/h)/|h|\} , \tag{23}$$

on $\zeta = e^{i\nu}$ for $\pi \geqslant \nu \geqslant 0$ and on the real axis for $1 \leqslant \zeta \leqslant 1$,

$$\mathrm{Im}\, f_1 = 0 . \tag{24}$$

Inspection of $h$ for $U > 1$ and $0 < \alpha < 1$ shows that the right-hand side of (23) is a smooth function of $\nu$ and can be expressed as a Fourier cosine series: $\Sigma_{n=0}^{\infty} d_n \cos n\nu$. It is not difficult to see that the coefficients $d_n \sim e^{-\delta n}$ as $n \to \infty$, where $\delta > 0$ and is related to $\alpha$ and $U$. From (23) and (24)

$$f_1 = \sum_{n=1}^{\infty} d_n \zeta^n . \tag{25}$$

Clearly, $f_1$ is analytic for $|\zeta| < e^{\delta}$. The second-order perturbation $f_2$ satisfies

$$\mathrm{Re}\, f_2 = -\frac{1}{|h|}\left[\mathrm{Re}\left(\zeta \frac{d}{d\zeta}\frac{f_1'}{h}\right) - \mathrm{Re}\left(\frac{f_1'}{h}\right)\mathrm{Re}\left(1 + \zeta \frac{d}{d\zeta}\ln h\right)\right] \tag{26}$$

on $\zeta = e^{i\nu}$, for $0 \leqslant \nu \leqslant \pi$ and on the real axis,

$$\mathrm{Im}\, f_2 = 0 . \tag{27}$$

Once again, the right-hand side of (26) is smooth and has a Fourier cosine series representation with coefficients decaying like $e^{-n\delta}$ for large $n$. At every stage, $f_n$ can be constructed recursively in terms of $f_{n-1}, f_{n-2}, \ldots, f_1$ and the power series coefficients of $f_n$ decay like $e^{-\delta n}$. Thus the higher-order perturbation terms are no more singular than the low-

er-order terms anywhere on or within the unit $\zeta$ circle and therefore the perturbation solution appears consistent for any $U$ and $\alpha$. The perturbation results indicate that a solution $f$ satisfying (14) and (18) exists for arbitrary $U$, $\alpha$, and $\epsilon$ over some range, which contradicts numerical evidence (presented later). A similar contradiction between numerics and perturbation appeared in the McLean–Saffman analysis of a finger. In the next two sections, we will produce evidence to show that for given $\alpha$ and $\epsilon$, solution $f$ satisfying (14) and (18) can exist only for isolated values of $U$ and therefore we deduce that the perturbation solution (22) is invalid unless some constraint is satisfied between $U$, $\alpha$, and $\epsilon$. When this constraint is not satisfied, indications are that the formal asymptotic series in (22) describes a function of $\zeta$ with a singular behavior in the flow domain. According to the arguments of Sec. II, this cannot correspond to the conformal mapping function that maps the $\zeta$ semicircle to the $z$ domain for the assumed fluid flow.

## IV. RELATED LINEAR PROBLEM

In this section, with a view to understanding the way in which (22) becomes invalid unless a proper constraint relation is satisfied, we will present a related linear problem for which a consistent formal perturbation solution exists even though the problem has no solution satisfying the given conditions. The relation between this problem and the original nonlinear problem satisfying (14) and (18) will be spelled out in Sec. V.

Let us consider the mathematical problem of finding an analytic function $f(\zeta)$ in the unit semicircle whose first two derivatives are continuous on the boundary and that satisfies conditions

$$\operatorname{Im} f = 0, \tag{28}$$

on the real axis and

$$\epsilon \operatorname{Re} \frac{d}{d\zeta}(\zeta^3 f') + 4 \operatorname{Re} f = \operatorname{Re} \zeta^2, \tag{29}$$

on $\zeta = e^{i\nu}$ for $0 \leqslant \nu \leqslant \pi$. From (28), it follows that on the real axis

$$\operatorname{Im}\left(\epsilon \frac{d}{d\zeta}(\zeta^3 f') + 4f - \zeta^2\right) = 0. \tag{30}$$

Equations (29) and (30) imply that

$$\epsilon \frac{d}{d\zeta}(\zeta^3 f') + 4f - \zeta^2 = 0, \tag{31}$$

for all $\zeta$.

Now, for small $\epsilon$, if we were to construct an asymptotic expression for solution $f$ satisfying (28) and (29) of the form (22), then we find $f_0 = \zeta^2/4$, $f_1 = -\zeta^3/2$, and so on. At every stage we are able to construct $f_n$ and the ratio of $f_n/f_m$ for fixed $n$ and $m$ $(n > m)$ stays bounded for all $|\zeta| \leqslant 1$. Thus the perturbation is consistent and one is lead to believe that that an analytic function $f$ exists within the unit $\zeta$ semicircle which satisfies conditions (28) and (29). However, this conclusion is erroneous as we will now demonstrate. Since we are looking for an analytic function $f(\zeta)$ which satisfies (28) on the real axis, we are guaranteed from the reflection principle that $f$ will have a power series convergent inside the unit circle. If $f$ is analytic within the unit circle, the expression on the left-hand side of (31) also must be. If we were to substitute that series into (31), the resulting series must be convergent within the unit circle and thus all the coefficients of different powers of $\zeta$ must be identically zero. This leads to a recurrence relation for the different coefficients and we obtain

$$f = \sum_{n=2}^{\infty} \frac{(-1)^n}{6}(n+1)!(n-1)!\frac{\epsilon^{n-2}}{4^{n-1}}\zeta^n, \tag{32}$$

which is a divergent series for all $\zeta \neq 0$. Thus we have a contradiction in the assumption that $f$ is analytic in the unit semicircle and its derivatives continuous on the boundary since such a solution must have a convergent power series representation within the unit $\zeta$ circle. Thus there is no solution for nonzero $\epsilon$. Specifically, we can conclude that $\zeta = 0$ is a singularity point for any $f$ satisfying (31). The divergence of the power series comes as no surprise since $\zeta = 0$ is an irregular singular point of the differential Eq. (31). Equation (32) is also the formal asymptotic series for $f$ in powers of $\epsilon$. However, this asymptotic series could not possibly be valid for all arguments of $\zeta$ in the neighborhood of zero since the function $f$ is singular at that point. We will now show that any solution $f$ to (31) possesses a singularity of exponential nature is the variable $(\epsilon\zeta)$ which does not appear in (32). By substituting $f = u^2 H(u)$ into Eq. (31), where $\zeta = 16/(\epsilon u^2)$, we obtain a nonhomogeneous Bessel's equation of second order for $H$. Using the well-known technique of variation of parameters, one obtains

$$f = \frac{16\pi i}{\epsilon^2}\left(u^2 H_2^2(u)\int_{\infty}^{u} H_2^1(t)t^{-3}\,dt - u^2 H_2^1(u)\int_{\infty}^{u} H_2^2(t)t^{-3}\,dt\right), \tag{33}$$

where the infinity in the limit is chosen to be on the positive real axis. When $\zeta$ is real and positive with zero argument, integration by parts and the use of the asymptotic properties of the Hankel functions of types 1 and 2 generate the same asymptotic series in $\epsilon$ as in (32). This asymptotic series will still be valid over regions of the complex $\zeta$ plane where the exponential terms generated by the integrals in (33) remain small. That such exponential terms exist can be easily demonstrated by computing the difference $f(\zeta e^{i2\pi}) - f(\zeta)$ when $\operatorname{Arg}(\zeta)$ is in $(0,2\pi)$, i.e., Arg $u$ between $-\pi$ and 0. To do this, we use the analytic continuation properties: $H_2^1(ue^{i\pi}) = -H_2^2(u)$ and $H_2^2(ue^{i\pi}) = 2H_2^2(u) + H_2^1(u)$ and deform the contours in the integrals in (33), noting with care that a change in the variable of integration changes the argument of infinity which must be taken into account. It is found that $f(\zeta e^{-i2\pi}) - f(\zeta) = ku^2 H_2^2(u)$, where $k$ is a nonzero constant. This difference is exponentially small when $\zeta$ or $\epsilon$ is small with $\operatorname{Arg}(\zeta)$ in $(0,2\pi)$. We note that this difference is a solution to the homogeneous problem and is singular at $\zeta = 0$. It may also be noted that if one were to add combinations of the solutions to the homogeneous problem to $f$ given in (33), we still cannot make $f$ single valued in the complex plane. Also, if one were concerned only with the boundary values of the analytic function $f$ on the circular boundary, as one is in the McLean–Saffman formulation, the periodicity condition on Re $f$ would be violat-

ed by an exponentially small amount. Thus we infer the existence of exponential terms in the asymptotics of $f$ which are not accounted for in a formal regular perturbation series in $\epsilon$. Any infinite truncation of the asymptotic series (32), however, does not reveal the existence of such terms. The consistency of any asymptotic series is usually considered to be a sign that a solution exists to a problem. Yet, this traditional wisdom is inapplicable here where we have shown that there are no solutions which satisfy the given conditions. In Secs. V and VI, we will present arguments to show that an analogous situation arises for the asymptotic perturbation series for $f$ satisfying (14) and (18).

## V. SMALL BUBBLE LIMIT

The limiting case of a small bubble that does not feel the effect of the cell walls corresponds to setting $\alpha$ to zero in (16). In (13), however, since $z$ scales with $\alpha$ in the limit of small bubbles, we do not set $\alpha$ to zero, but take the leading order behavior. We notice that there is a trivial solution, $f=\epsilon$, $U=2$ to the nonlinear equations (14) and (18) in this limit. This corresponds to a small circular bubble. Now, if $U$ were a free parameter, as our formal perturbation series expansion in $\epsilon$ suggested, we ought to be able to find other solutions in the neighborhood of $U=2$ for any $\epsilon$. We therefore expect to be able to construct a perturbation series for the solution for small $\beta$, where $\beta=U-2$. Thus we seek a solution

$$f=\sum_{n=0}\beta^n g_n\,. \tag{34}$$

Expansion of $h$ in powers of $\beta$ and substitution of $f$ and $h$ into (14) and (18) leads to equations for $g_n$. Clearly, $g_0=\epsilon/2$ and $g_1$ satisfies

$$\mathrm{Re}(\epsilon\zeta^3 g_1''+3\epsilon\zeta^2 g_1'+4g_1+\epsilon-3\epsilon\zeta^2)=0\,, \tag{35}$$

on $\zeta=e^{i\nu}$ for $\nu$ in $[0,\pi]$, and on the real axis, $\mathrm{Im}(g_1)=0$. These two conditions imply that for all $\zeta$,

$$\epsilon\zeta^3 g_1''+3\epsilon\zeta^2 g_1'+4g_1=-\epsilon+3\epsilon\zeta^2\,. \tag{36}$$

In view of the linearity of the problem and what was established in the last section, it is clear that there can be no analytic function $f$ in the unit semicircle with its first two derivatives continuous on its boundaries which satisfy the above equations. Failure to construct a perturbation solution for small $\beta$ suggests that $U=2$ is an isolated value for which solutions $f$ satisfying (14) and (18) exist. Thus, for any given $\alpha$ and $\epsilon$, it is expected that there will be a constraint $U=U(\alpha,\epsilon)$. We now obtain an explicit constraint relation in the case when $\alpha$ is small, but $\epsilon$ is of order 1. We assume

$$f=\sum_{n=0}\alpha^{2n}f_n \tag{37}$$

and

$$U=2+\sum_{n=1}\alpha^{2n}U_n(\alpha,\epsilon)\,. \tag{38}$$

We also expand $h$ in (16) in powers of $\alpha^2$ assuming $U$ to be of the above form. Substitution into (14) and (18) once again leads to a differential equation:

$$\epsilon\zeta^3 f_1''+3\epsilon\zeta^2 f_1'+4f_1=-\epsilon U_1+\epsilon\zeta^2(3U_1+2)\,, \tag{39}$$

which will have a solution only when $U_1=-2/3$. We have $f_1=\epsilon/6$. For the next order term, we get

$$\epsilon\zeta^3 f_2''+3\epsilon\zeta^2 f_2'+4f_2 = \epsilon\left[-U_2+(3U_2-\tfrac{2}{3})\zeta^2-\tfrac{2}{3}\zeta^4\right]\,. \tag{40}$$

If we substitute a power series in $\zeta$ for $f_2$ in the above equation, we obtain equations relating different coefficients. Once the coefficients are found, it is easy to see that the resulting series is divergent unless

$$U_2=2/9+4/(135\epsilon^2)\,, \tag{41}$$

for which the power series terminates. We obtain

$$f_2=-\epsilon[1/18+1/(135\epsilon^2)]+\zeta^2/(45\epsilon)-2\zeta^3/(45)\,. \tag{42}$$

Thus we obtain a perturbation solution for $f$ and $U(\alpha,\epsilon)$ in powers of $\alpha^2$. It is clear from (41) and (42), however, that these solutions and constraints are not uniformly valid for all $\epsilon$ since both $f_2$ and $U_2$ blow up when $\epsilon$ goes to zero. It is found that for $\epsilon$ of order 1, the above perturbation solution is in agreement with the numerically obtained $f$ and $U$ for the full nonlinear problem with the error being sixth order in $\alpha$. Construction of a uniformly valid expansion for all $\epsilon$ appears to be far from straightforward. The recent work of Shraiman, Combescot *et al.*, and Hong and Langer dealing with a finger, as noted earlier, may be relevant to the construction of such a uniformly valid expansion. This will not be addressed in this paper. Nonetheless, our ability to construct an explicit constraint solution for at least one branch of bubble solutions for some range in $\epsilon$, $\alpha$ space is a clear indication that the introduction for surface tension removes the degeneracy of the Taylor–Saffman solutions. When the bubble is large, it seems improbable that an explicit constraint relation can be constructed in view of the complexity of the equations. However, our findings that a regular perturbation series in powers of $\epsilon$ leads to spurious results for the case of a small bubble because of the presence of exponentially small terms leads one to believe that the same thing is true for the case of larger bubbles. In the next section, we construct a modified perturbation solution for small $\epsilon$ which strongly suggests that this is the case.

## VI. MODIFIED PERTURBATION PROCEDURE

Instead of assuming a perturbation series (22) for $f$, we only assume that the leading order term $f_1$ is small when $\epsilon$ is small. Equation (24) will clearly be satisfied by $f_1$. On $\zeta=e^{i\nu}$ for $0\leqslant\nu\leqslant\pi$, linearization of (18) gives us

$$\epsilon\,\mathrm{Re}\,\zeta\frac{d}{d\zeta}\left(\frac{f_1'}{h}\right)+|h|\mathrm{Re}f_1=-\epsilon\left[1+\mathrm{Re}\left(\frac{\zeta h'}{h}\right)\right]\,. \tag{43}$$

This equation is solved numerically as discussed in Sec. IV. No solution to this could be found when $U$ is arbitrarily specified along with $\alpha$ and $\epsilon$. There is a necessary constraint between $U$, $\alpha$, and $\epsilon$ even for this linear problem in order that a solution exist. It is found that the solution $f_1$ and $U$ for given $\alpha$ and $\epsilon$ agreed well with the solution to the full nonlin-

ear problem when $\epsilon$ was small. The disagreement is $O(\epsilon^2)$.

Thus the retention of the highest derivative term in the perturbation equation leads to a constraint condition for $U$ which is absent when all the derivative terms are dropped. This happens in spite of the fact that all the boundary conditions are satisfied by the original perturbation terms $f_n$ in Sec. III. In order to see how the modified first-order perturbation equation (43) can lead to a constraint, we now show that (43) is equivalent to a Fredholm integral equation of the second kind by substituting $p(\nu) = \mathrm{Im}(f_1'/h)$ on $\zeta = e^{i\nu}$. By integrating (43), with respect to $\nu$, we find

$$\begin{aligned}\epsilon p(\nu) &+ \int_0^\nu d\chi |h(e^{i\chi})| \int_0^\chi d\varphi \,\mathrm{Re}\,[ie^{i\varphi}h(e^{i\varphi})]q(\varphi) \\ &- \int_0^\nu d\chi\, |h(e^{i\chi})| \int_0^\chi d\varphi \,\mathrm{Im}\,[ie^{i\varphi}h(e^{i\varphi})]p(\varphi) \\ &= -q_0 \int_0^\nu d\chi\, |h(e^{i\chi})| \int_0^\chi d\varphi \,\mathrm{Re}\,[ie^{i\varphi}h(e^{i\varphi})]d\varphi \\ &\quad -f_1(1)\int_0^\nu d\chi\, |h(e^{i\chi})| \\ &\quad -\epsilon \int_0^\nu d\chi \,\mathrm{Re}\left(1 + e^{i\chi}\frac{h'}{h}(e^{i\chi})\right), \end{aligned} \tag{44}$$

where

$$q_0 = f_1'(0)/h(0)$$

and

$$q(\nu) = \frac{1}{2\pi} \fint_0^\pi d\varphi\, p(\varphi) \left[\cot\left(\frac{\varphi-\nu}{2}\right) + \cot\left(\frac{\varphi+\nu}{2}\right)\right] \tag{45}$$

and is related to $\mathrm{Re}(f_1'/h)$ by the additive term $q_0$. From (44) and (45) and the switching of the order of integration (which can be shown to be valid under reasonable conditions on $p$) we obtain a Fredholm integral equation of the second kind of the form

$$\epsilon p(\nu) + \int_0^\pi K(\nu,\varphi)p(\varphi)d\varphi = \mathscr{R}[\epsilon, q_0, f_1(1), U, \alpha, \nu], \tag{46}$$

where $K(\nu,\varphi)$ is a logarithmically singular kernel and $\mathscr{R}$ is the right-hand side of (44) which is a function of the variable $\nu$ as well as the parameters $q_0, f_1(1), U, \epsilon$, and $\alpha$. Since $f'/h$ is analytic the unit $\zeta$ circle and $p$ and $q$ are the imaginary and real parts of that analytic function, the condition that $f'/h$ equals zero at $\zeta = \pm\alpha$ implies two conditions involving $q_0$ and integrals involving $p(\nu)$. Further, $p(\nu)$ is an odd periodic continuous function of $\nu$ and therefore $p(\pi) = 0$ is an additional condition. [It may be noted that (46) automatically implies that $p(0) = 0$.] Thus we have three constraint conditions that have to be satisfied by solution $p(\nu)$ to (46). For arbitrarily specified $U$, $\alpha$, and $\epsilon$, we cannot expect that there can be any choice of $f_1(1)$ and $q_0$ for which the three constraint conditions can be satisfied unless these conditions are not independent. We are unable to rigorously prove that these conditions are independent; however, based on numerical evidence [obtained by solving the equivalent problem of finding $f_1$ satisfying (43)], we conclude that this is the case. Thus, for given $\epsilon$ and $\alpha$, if we treat $q_0, f_1(1)$, and $U$ as unknowns, along with $p(\nu)$, we can expect that the three constraint conditions will be satisfied by the solution $p(\nu)$.

## VII. LIMIT OF LARGE SURFACE TENSION

In order to investigate the limit of large $\epsilon$, it is convenient to consider the original boundary condition (11) on the bubble boundary which in a nondimensional form becomes

$$\phi + Ux = \mathbb{B}\kappa + \text{const}, \tag{47}$$

where $\kappa = 1/R$ is the curvature and $\mathbb{B} = Tb^2/12\mu$. Differentiating (47) with respect to $\phi$ on the boundary and using $\kappa = d\theta/ds$ and $dz/dW = e^{i\theta}/q$, where $s$ is the arclength measured from the front stagnation point, $q$ is the magnitude of velocity, and $\theta$ is the angle between the tangent on the bubble boundary and the $x$ axis, one finds

$$\kappa + U\frac{d}{d\phi}\sin\theta = \frac{\mathbb{B}}{2}\frac{d}{d\phi}\kappa^2. \tag{48}$$

The above form of the boundary condition was first given by Kadanoff[10] and he used it to deduce that solutions for a finger in a Hele–Shaw cell could not exist if $\mathbb{B}/U$ is larger than some critical value. In our case, the results will be derived by using both forms (47) and (48); but a few steps closely follow Kadanoff's original argument for a finger. From (47), we deduce that

$$\phi_M - \phi_m + U(x_M - x_m) = \mathbb{B}(\kappa_M - \kappa_m), \tag{49}$$

where subscripts $M$ and $m$ refer to points on the bubble contour where the maximum and minimum values of $\kappa$ are attained. Integrating (48), we obtain

$$U(\sin\theta_M - \sin\theta_m) + \int_{\phi_m}^{\phi_M} \kappa\, d\phi = \frac{\mathbb{B}}{2}(\kappa_M^2 - \kappa_m^2). \tag{50}$$

Now, the quantity on the right side of Eq. (49) is positive and so in general we have the inequality

$$\phi_A - \phi_B + UL_x > \mathbb{B}(\kappa_M - \kappa_m) > 0, \tag{51}$$

where subscripts $A$ and $B$ refer to the rear and front stagnation point values and $L_x$ is the length of the bubble (in the $x$ direction). Equation (51) will be used to show that for a given area, if we assume that $U < 2$ and that $L_x$ does not grow with $\mathbb{B}$, then the circle is the only possible contour for a bubble in the limit of $\mathbb{B}$ tending to infinity. However, before we proceed to the proof, it is worthwhile noting that if we assume $\kappa \geqslant 0$ everywhere on the bubble, then we have a sharper form of inequality in (51). For that case, two subcases are possible. First, if $\phi_M - \phi_m \geqslant 0$, then the term $UL_x$ on the left-hand side of inequality (51) is not necessary since $x_M - x_m$ will then be negative in Eq. (49). For the second subcase, $\phi_M - \phi_m < 0$. Also, we note that in order that the bubble contour turn around an angle of 180°, without hitting the wall located at $y = 1$, we must have $\kappa_M > 1$ and so for the case of positive curvature $\kappa_M + \kappa_m > 1$. Then it follows from (50) that

$$4U \geqslant \mathbb{B}(\kappa_M^2 - \kappa_m^2) \geqslant \mathbb{B}(\kappa_M - \kappa_m) \geqslant 0. \tag{52}$$

Combining the two subcases, we have that for a bubble of positive curvature

$$\phi_A - \phi_B + 4U \geqslant \mathbb{B}(\kappa_M - \kappa_m) \geqslant 0, \tag{53}$$

which is different from (51) in that it does not involve the length of the bubble. We now find an *a priori* estimate of how large $\phi_A - \phi_B$ can be in terms of the area of the bubble $J$ and its speed $U$. From (12) and (21), it follows that

$$J\frac{U^2}{2} = \phi_A - \phi_B + \frac{4}{\pi}(U-1)\log\left(\frac{(1+\alpha)^2}{(1+\alpha^2)}\right) + \frac{2}{\pi}\alpha(U-1)[f(\alpha) - f(-\alpha)]\,. \tag{54}$$

Since $\mathrm{Re}\,f$ is a harmonic function in the unit $\zeta$ circle, we can use Poisson's integral formula (for even boundary data) to get

$$f(\alpha) - f(-\alpha) = \int_0^\pi d\nu\, P(\alpha,\nu)[\mathrm{Re}\,f(e^{i\nu}) - \mathrm{Re}\,f(e^{i(\pi-\nu)})], \tag{55}$$

where $P$ is the Poisson's kernel given by

$$P(\alpha,\nu) = (1-\alpha^2)/[\pi(1-2\alpha\cos\nu+\alpha^2)]\,. \tag{56}$$

We notice that $P$ is always positive and its integral with respect to $\nu$ over the interval $(0,\pi)$ is 1. Further, from Eqs. (17) and (18), we can relate $\mathrm{Re}\,f$ to the curvature $\kappa$. It is easily seen from (55) that $f(\alpha) - f(-\alpha)$ can be bounded in terms of the maximum difference of curvatures, i.e., $\kappa_M - \kappa_m$. Using this bound, it follows from (54), (55), and (56) that

$$\phi_A - \phi_B < \frac{JU^2}{2} + \frac{4(U-1)}{\pi}\log\left(\frac{(1+\alpha)^2}{(1+\alpha^2)}\right) + (U-1)\mathbb{B}(\kappa_M - \kappa_m)\,. \tag{57}$$

Using the upper bound in (57), we find from (53) that for the case of positive curvature

$$\frac{JU^2}{2\mathbb{B}} + \frac{4U}{\mathbb{B}} + 4\frac{(U-1)}{\pi\mathbb{B}}\log 2 \geqslant (2-U)(\kappa_M - \kappa_m)\,. \tag{58}$$

For the general case when only (51) is applicable we find from (57) that

$$\frac{JU^2}{2\mathbb{B}} + L_x\frac{U}{\mathbb{B}} + 4\frac{(U-1)}{\pi\mathbb{B}}\log 2 \geqslant (2-U)(\kappa_M - \kappa_m)\,. \tag{59}$$

If we now assume that $U<2$ and that it does not approach 2 as $\mathbb{B}$ tends to infinity (an assumption backed by numerical results), then in the limit of infinite $\mathbb{B}$ for finite specified area $J$, $\kappa_M$ approaches $\kappa_m$ for the case of positive curvature. In general, however, when the less strict inequality (59) is valid, we find that we need to make an additional *a priori* assumption that $L_x$ does not grow at a faster rate than $\mathbb{B}$, as $\mathbb{B}$ tends to infinity in order that $\kappa_M$ tend to $\kappa_m$. Thus the circle is the only possible contour for a bubble of fixed area if the curvature of the limiting solution is assumed non-negative. We are unable to rigorously rule out the possibility of existence of bubbles with negative curvatures on part of the bubble boundary which grow at least linearly with $\mathbb{B}$, as $\mathbb{B}$ tends to infinity. However, we are able to deduce some properties of these negative curvature solutions from Eqs. (48) and (49). In the limit of infinite $\mathbb{B}$, the negative curvature can only be limited to a neighborhood of the front stagnation point. Thus the only way $L_x$ could grow is for the limiting bubble to be indefinitely deformed towards the oncoming flow (in the frame of the bubble). There are elongated bubbles of this type (see Fig. 6) for moderate values of $\mathbb{B}$. Whether these bubbles continue to elongate indefinitely for larger and larger $\mathbb{B}$ as the area $J$ is held fixed still remains an open question. In the event that this is a possibility, Saffman[10] points out that such a bubble would correspond to two semi-infinite fingers located symmetrically about $y=0$. Our method of solution cannot accurately calculate these sharp curvature solutions. It is therefore unclear whether the circle is the only possible limiting bubble shape when we allow for the possiblity of negative $\kappa$ on parts of the bubble contour. In the case when the area of the bubble is bigger than $\pi$, clearly the bubble cannot be fitted into the channel as a circle. In that case the circular bubble is no longer a possibility and it is not known whether any steady state bubble solutions are possible. There are, of course, steady nonbubble solutions where the less viscous fluid fills up a finite part of the whole channel and the interface satisfies equations given in Sec. 6 of McLean–Saffman's paper. These form a degenerate set and their relevance to the physical problem of Hele–Shaw cell flows is unclear.

## VIII. NUMERICAL PROCEDURE

It is convenient to use the representation

$$f = \sum_{m=0}^{\infty} a_n \zeta^n \tag{60}$$

for bubbles that are not too elongated along the $x$ axis. In view of (14), $a_n$'s are all real and from the regularity features of the conformal map $z(\zeta)$, it follows that if the bubble is assumed to have a smooth boundary, then $a_n$ decreases exponentially with $n$ for large $n$. The coefficient of $n$ in the exponent depends on the shortest distance of a singularity of $f$ from the unit $\zeta$ circle. This becomes rather small when the bubble contour develops regions of large curvature. Thus, if we were to truncate (60), a lot of terms would be needed to approximate $f$ accurately. We abandon the representation (60) in extreme cases and instead use

$$\mathrm{Re}\,f = \sum_{n=0}^{\infty} \hat{a}_n \cos n\hat{\nu}\,, \tag{61}$$

on $\zeta = e^{i\nu}$ for $0 \leqslant \nu \leqslant \pi$

$$\nu = \hat{\nu} - \gamma \sin 2\hat{\nu}\,, \tag{62}$$

where $\gamma$ is a number determining the stretching and is chosen in the interval $[0,1/2]$. For bubbles which are very long and elongated, we used $\gamma = 0.499$. If the representation (61) is used, $\mathrm{Im}\,f$ is determined by the Hilbert transform

$$\mathrm{Im}\,f = \frac{1}{2\pi}\int_0^\pi d\hat{\nu}'\,\frac{d\nu'}{d\hat{\nu}'}\left[\cot\left(\frac{\nu-\nu'}{2}\right) + \cot\left(\frac{\nu+\nu'}{2}\right)\right] \times [\mathrm{Re}\,f(\hat{\nu}') - \mathrm{Re}\,f(\hat{\nu})]\,, \tag{63}$$

where the integrand has been desingularized and $\nu$, $\nu'$ are related to $\hat{\nu}$, $\hat{\nu}'$ through (62). It is possible to use finite differences on point values of $\mathrm{Re}\,f$ and $\mathrm{Im}\,f$ to compute the derivatives $f'$ and $f''$. However, once the stretched variable $\nu'$ is introduced, the number of terms necessary in the truncated representation (61) is found to be fairly small most of the time, and so the derivatives of $f$ can be calculated accurately

in a more efficient manner by first finding the coefficients $\hat{b}_n$ in the representation

$$\mathrm{Im}\, F(\hat{v}) = \sum_{n=1}^{\infty} \hat{b}_n \sin n\hat{v}\,. \tag{64}$$

Now $f, f'$, and $f''$ on $\zeta = e^{iv}$ can be expressed in terms of $\mathrm{Re}\, f$ and $\mathrm{Im}\, f$ and its first two derivatives with respect to $\hat{v}$. The representation in (61)–(64) usually needs more work from a computational viewpoint since integration is involved in (63). However, in the case of bubbles with sharp curvature near the centerline of the channel, we need much fewer terms in (61) than in (60) for accurate representation of $f$ and the extra work involved in (63) is compensated for.

The numerical procedure is especially simple for the representation (60), which is truncated to $N$ terms so that $N$ is a multiple of 2. At uniformly spaced out points on the arc of the $\zeta$ semicircle, of the form $v_k = (k-1)\pi/N$, $k = 1,2,\ldots, (N+1)$, Eq. (18) is satisfied. We have a system of $(N+1)$ nonlinear equations for the $(N+1)$ unknowns $U/V, a_0, a_1,\ldots, a_{N-1}$, where $\epsilon$ and $\alpha$ are given. Newton iteration is then used to find these unknowns and the solution is said to have converged when the maximum residual error is less than $10^{-12}$. Consistency of solution is then checked by doubling $N$ and carrying out the Newton iterative procedure once again. Calculation of the residual for each iteration is expedited by the use of the discrete fast Fourier transform to calculate $f, f'$, and $f''$ for given $a_0, a_1,\ldots, a_{N-1}$. The same procedure is used to find the solution $f_1$ to the modified perturbation equation (43).

For the representation (61), which is truncated to $N$ terms, we take $(N+1)$ collocation points of the form $\hat{v}_k = (k-1)\pi/N$, $k = 1,2,3,\ldots, (N+1)$ and satisfy Eq. (18) for the $(N+1)$ unknowns $U/V, \hat{a}_0, \hat{a}_1,\ldots, \hat{a}_{N-1}$. This is again done by Newton iteration. However, we now have to use (63) and find $\hat{b}_n$ in (64) since both sets of coefficients $\hat{a}_n$ and $\hat{b}_n$ are necessary to calculate $f, f'$, and $f''$ in (18). This is done in the following manner.

For given $\hat{a}_0, \hat{a}_1,\ldots, \hat{a}_{N-1}$, a fast Fourier cosine transform is used to calculate $\mathrm{Re}\, f$ at $(N_H+1)$ uniformly spaced out points of the form $\hat{v}_j = (j-1)\pi/N_H$, where $j = 1,2,\ldots, N_H+1$. Here $N_H$ is chosen to be a multiple of $N$ so that the set $\{\hat{v}_j\}_{j=1}^{N_H+1}$ includes the set of points $\{\hat{v}_k\}_{k=1}^{N+1}$. Using these $N_H+1$ point values of $\mathrm{Re}\, f_1$ trapezoidal rule gives the approximate value of the integral in (63) for the $N-1$ points $\{\hat{v}_k\}_{k=2}^{N}$. For the terms in the finite sum approximation of (63) of the form 0/0, we replace it by the average value of the integrand at the two adjacent points. It is not necessary to calculate $\mathrm{Im}\, f$ for $\hat{v}_1$ and $\hat{v}_{N+1}$ since it is known to be zero at those points. After calculating $\mathrm{Im}\, f$ at the uniformly spaced points of the form $\{\hat{v}_k\}_{k=1}^{N+1}$, a fast Fourier inverse sine transform is used to calculate $N$ terms $\hat{b}_n$ in (64). We can then use (61), (62), and (64) to calculate $f, f'$, and $f''$ at the $(N+1)$ points of collocation.

For small $\alpha$ and $\epsilon$, initial guesses of $U = 2$ and $a_i$ all zero were taken for the Newton iteration. Using a standard continuation procedure in parameters $\alpha$ and $\epsilon$, good initial guesses for other $\alpha$ and $\epsilon$ were obtained. The condition number and the determinant of the Jacobian were each monitored in the Newton iteration procedure and each remained of the same order of magnitude between iterations. Further, the determinant never changed sign. These features were independent of $N$. This suggests that the Jacobian is not singular and that $U$ together with $f$ (or $f_1$) can be treated as unknowns in (18) [or (43)]. Our efforts to find solutions to (14) and (18) and $U$, $\alpha$, and $\epsilon$ specified failed even for very small $\epsilon$ with zero initial guess unless $U$ attained some specific isolated values depending on $\alpha$ and $\epsilon$. In fact if $U$ is taken to be only very slightly different from those isolated values, Newton's iteration either failed to converge or gave values of $a_0, a_1,\ldots, a_{N-1}$ that were inconsistent when $N$ was doubled. All these features were also observed for the solution $f_1$ to (43). Thus there seems to be little doubt that the degeneracy of Taylor–Saffman bubble solutions is removed by the introduction of surface tension.

The procedure outlined in the last paragraph only gives one branch of solution, which we call the main branch. In order to find other possible solutions $f$ satisfying (14) and (18), we first consider a procedure to find all solutions to the modified first-order perturbation term $f_1$ satisfying (43). For small $\epsilon$, these solutions can be taken as initial guesses in the Newton iterative procedure for finding $f$ that satisfies (14) and (18).

Instead of taking $f_1$ as our unknown in (43), let $g \equiv f_1'/h$ be taken as the unknown function. Then

$$f_1(\zeta) = f_1(0) + \int_0^{\zeta} h(\zeta) g(\zeta)\, d\zeta\,, \tag{65}$$

where $g(\zeta)$ has the representation

$$g(\zeta) = \sum_{n=0}^{\infty} c_n \zeta^n\,, \tag{66}$$

with $c_n$'s all real. Besides satisfying Eq. (43) on $\zeta = e^{iv}$ for $0 \leqslant v \leqslant \pi$, the relation between $f_1$ and $g$ implies the two conditions on $g$

$$g(+\alpha) = 0\,, \tag{67}$$

$$g(-\alpha) = 0\,. \tag{68}$$

However, in the procedure to find all branches of solution satisfying (43), we will relax condition (68) and take $U$ together with $\alpha$ and $\epsilon$ as specified parameters. In some sense, the idea is similar to that of Vanden-Broeck[6] who presents a systematic procedure to find other steady finger solutions. We truncate (66) to $(N+1)$ terms. By using the fast Fourier transform, $g$ is evaluated at $2N$ uniform spaced out points on the $\zeta$ circle of the form $e^{iv_l}$, where $v_l = (l-1)\, 2\pi/(2N)$, $l = 1,\ldots,2N$. The product $gh$ is then evaluated at these $2N$ points and the fast Fourier inverse transform is used to compute the $N$ coefficients of an $N$ th-order interpolating polynomial in $\zeta$. In general, these polynomial coefficients are unrelated to the Taylor series coefficients of $f_1$ since such a series cannot be convergent on the unit $\zeta$ circle in view of the singularity of $gh$ at $\zeta = -\alpha$ which is not removable unless the condition (68) is satisfied. Nevertheless, the polynomial expression for $f_1$ is used to calculate the integral in (65) in the Fourier space. Since at the end, our purpose is to determine a genuine solution of (43) for which the corresponding $g$ satisfies both conditions (67) and (68), we will not be bothered with the physical or mathematical relevance of the

procedure since it is found to work. The $N$ polynomial coefficients for $f_1$ are used to calculate $f$, $f'$, $f''$ at $N+1$ uniformly spaced out points of the form $\nu_k = (k-1)\pi/N$, $k = 1,2,...,(N+1)$. Thus the residual in (43) is calculated at $N+1$ points for given $c_0, c_1,..., c_N$ in (66). Including (67), we have $(N+2)$ equations for $(N+2)$ unknowns $f_1(0), c_0, c_1,..., c_N$ which is solved in one Newton iteration since the system is linear. This is done for different $U$ for fixed $\alpha$ and $\epsilon$ and the residual error in (68) monitored. When this is found to be zero, consistency of such solutions is checked by doubling $N$ and if they are consistent, the corresponding values of $U$ and Taylor series coefficients are used as initial guesses in the Newton iterative procedure to find $f$ satisfying (14) and (18). Using this procedure for $\epsilon = 0.1$ and $\alpha = 0.5$, we obtained just one other branch of solution to our full nonlinear problem, which we call the extraordinary branch.

## IX. NUMERICAL RESULTS

As mentioned in the last section, we found two branches of solution; the first one we call the main branch asymptotes to the McLean–Saffman finger solutions when $\alpha$ tends to 1 and seems to exist for all positive $\epsilon$ for any fixed $\alpha$ in the range (0,1). However, for fixed specified areas bigger than $\pi$, according to the arguments of Sec. VI, this branch (for which the bubble contour has positive curvature) cannot exist when $\epsilon$ is larger than some critical value. This is consistent with Kadanoff's findings for a finger. Table I lists the bubble velocity $U$, the $x$ distance between the front and rear stagnation point $x_B - x_A$, the half-width of the bubble $\lambda$, and the area $J$ for different $\alpha$ and $\epsilon$ for the main branch of solution. For fixed $\epsilon$, as $\alpha$ increases from 0 to 1, the bubble increases in size and elongates along the $x$ axis and $U$ decreases from a maximum of 2 for small bubbles to a minimum of 1 for $\alpha \to 1$. For fixed $\alpha$, as $\epsilon$ tends to zero, the bubble velocity $U$ tends to 2. This is remarkable since Taylor and Saffman[2] found that $U = 2$ minimizes the product $U\lambda$ for their exact solutions corresponding to zero surface tension for any size of the bubble. How their minimization principle relates to the introduction of surface tension is a fascinating though apparently difficult question. The bubble shape is the upper half-plane for $\epsilon = 0.2$ and $\alpha = 0.99$ is compared in Fig. 4 with the McLean–Saffman finger corresponding to the same value of $\epsilon$. (The equality $\lambda = 1/U$ was used to find that $\epsilon = 0.2$ corresponds to $\kappa = 1.79$ in the McLean–Saffman notation.) The agreement is almost perfect for the front of the bubble. This provides a check for the code. For fixed $\alpha$, as $\epsilon$ increases from 0 to $\infty$, the bubble gets more and more circular, which is consistent with the arguments of Sec. VII. In Fig. 5, the contour for the upper half of the bubble is shown for different $\epsilon$ and $\alpha = 0.99$. It is found that the closer $\alpha$ is to 1, the larger is the value of $\epsilon$ for which a circular contour is approached. The velocity $U$ approaches some number between 2 and 1 depending on $\alpha$. The transcendental equation determining the limiting $U(\alpha)$ is found by equating $J$ in (21) to $\pi(x_B - x_A)^2$. From (12) and (47),

$$x_B - x_A = \frac{\phi_A - \phi_B}{U} = \frac{4(U-1)}{\pi U} \log\left(\frac{1+\alpha}{1-\alpha}\right). \qquad (69)$$

We note that there is no dependence of $J$ on $f$ since for a circular bubble there is no difference between $f(\alpha)$ and $f(-\alpha)$.

Table II shows results for the extraordinary solution branch. The bubbles corresponding to this branch are, in the range of numerical calculations, elongated along the $y$ direction relative to the $x$ direction. For fixed $\epsilon$, as $\alpha$ increases, $x_B - x_A$ decreases and the half width $\lambda$ increases while the curvature on parts of the bubble contour becomes negative beyond some critical value. For fixed $\alpha$, as $\epsilon$ is increased, the curvature on parts of the bubble becomes negative and the bubble becomes more and more deformed towards the $x$ axis. Figures 6 and 7 show the upper half of the bubble con-

TABLE I. Various constants characterizing the bubbles of the main branch for different $\alpha$ and $\epsilon$.

| | | Properties of the main branch of solutions | | | |
|---|---|---|---|---|---|
| $\alpha$ | $\epsilon$ | $U$ | $x_B - x_A$ | $\lambda$ | $J$ |
| 0.02 | 0.01 | 1.999 8 | 0.025 465 | 0.012 732 | 0.000 5093 |
| 0.1 | 0.01 | 1.997 9 | 0.127 615 | 0.063 518 | 0.012 733 |
| 0.2 | 0.01 | 1.994 6 | 0.257 42 | 0.126 09 | 0.050 956 |
| 0.5 | 0.01 | 1.981 285 | 0.692 80 | 0.297 96 | 0.325 19 |
| 0.81 | 0.01 | 1.964 270 | 1.408 927 | 0.441 305 | 1.000 3 |
| 0.99 | 0.01 | 1.953 081 | 3.288 9 | 0.508 74 | 2.926 9 |
| 0.02 | 0.1 | 1.999 7 | 0.025 465 | 0.012 732 | 0.000 5093 |
| 0.2 | 0.1 | 1.977 8 | 0.255 239 | 0.127 08 | 0.050 95 |
| 0.5 | 0.1 | 1.916 15 | 0.669 24 | 0.308 34 | 0.324 57 |
| 0.81 | 0.1 | 1.839 6 | 1.312 68 | 0.472 4 | 0.992 80 |
| 0.99 | 0.1 | 1.790 67 | 2.981 8 | 0.555 1 | 2.887 7 |
| 0.2 | 0.2 | 1.976 76 | 0.254 84 | 0.127 28 | 0.050 948 |
| 0.5 | 0.2 | 1.873 4 | 0.652 96 | 0.315 52 | 0.323 71 |
| 0.81 | 0.2 | 1.744 8 | 1.233 | 0.501 2 | 0.978 74 |
| 0.99 | 0.2 | 1.677 01 | 2.738 6 | 0.598 58 | 2.816 97 |
| 0.5 | 0.3 | 1.857 6 | 0.646 67 | 0.318 24 | 0.323 29 |
| 0.81 | 0.3 | 1.674 4 | 1.167 2 | 0.523 85 | 0.962 34 |
| 0.99 | 0.3 | 1.589 | 2.532 4 | 0.644 5 | 2.727 1 |
| 0.5 | 0.5 | 1.848 96 | 0.643 16 | 0.319 74 | 0.323 03 |
| 0.99 | 0.5 | 1.420 6 | 2.072 4 | 0.738 | 2.430 81 |
| 0.50 | 1.0 | 1.845 3 | 0.641 66 | 0.320 38 | 0.322 915 |
| 0.81 | 1.0 | 1.610 1 | 1.099 9 | 0.545 05 | 0.941 718 |
| 0.99 | 1.0 | 1.310 6 | 1.686 | 0.797 3 | 2.110 79 |

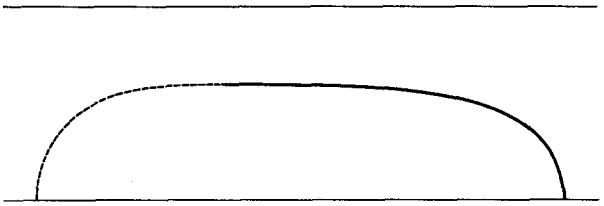

FIG. 4. The upper half of the bubble contour for $\epsilon = 0.2$ and $\alpha = 0.99$ is compared against the McLean–Saffman finger shape for equivalent value of surface tension parameter ($\kappa = 1.79$, in their notation). The dark line indicates overlap between the two contours.

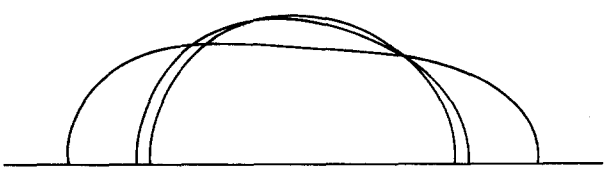

FIG. 5. Upper half of the bubble contour for $\alpha = 0.99$ and $\epsilon = 0.3$, 0.7, and 1.5. Larger $\epsilon$ corresponds to a more circular bubble. The straight lines correspond to the wall at $y = +a$ and the line of symmetry at $y = 0$.

TABLE II. Constants corresponding to the bubbles of the extraordinary branch.

| | | Properties of the extraordinary branch | | | |
|---|---|---|---|---|---|
| $\alpha$ | $\epsilon$ | $U$ | $x_B - x_A$ | $\lambda$ | $J$ |
| 0.02 | 0.01 | 1.858 9 | 0.023 535 | 0.013 697 | 0.000 5064 |
| 0.1 | 0.01 | 1.851 0 | 0.117 46 | 0.068 5576 | 0.012 650 |
| 0.2 | 0.01 | 1.825 3 | 0.233 41 | 0.137 69 | 0.050 490 |
| 0.5 | 0.01 | 1.615 49 | 0.532 92 | 0.365 38 | 0.306 78 |
| 0.78 | 0.01 | 1.204 637 | 0.450 476 | 0.697 038 | 0.507 15 |
| 0.80 | 0.01 | 1.153 099 | 0.366 01 | 0.738 893 | 0.444 29 |
| 0.82 | 0.01 | 1.127 | 0.323 5 | 0.767 4 | 0.415 3292 |
| 0.84 | 0.01 | 1.110 9 | 0.298 1 | 0.790 89 | 0.401 3189 |
| 0.50 | 0.0002 | 1.861 4 | 0.647 316 | 0.317 147 | 0.323 40 |
| 0.50 | 0.004 | 1.795 355 | 0.619 676 | 0.328 812 | 0.320 98 |
| 0.5 | 0.1 | 1.714 2 | 0.581 18 | 0.343 73 | 0.316 13 |
| 0.5 | 0.15 | 1.568 479 | 0.495 164 | 0.371 719 | 0.299 96 |
| 0.5 | 0.18 | 1.387 8513 | 0.342 467 | 0.407 060 | 0.257 75 |
| 0.5 | 0.2 | 1.307 22 | 0.245 69 | 0.420 57 | 0.225 90 |
| 0.50 | 0.22 | 1.261 5 | 0.176 89 | 0.426 01 | 0.202 70 |
| 0.50 | 0.24 | 1.232 26 | 0.124 48 | 0.427 87 | 0.185 47 |

tour shapes corresponding to the extraordinary branch of solution. For the bubble in Fig. 6, $\alpha$ is held fixed at 0.5. The four contours correspond to $\epsilon = 0.15$, 0.2, 0.22, and 0.24 with the more deformed ones corresponding to larger $\epsilon$. In Fig. 7, $\epsilon$ is held fixed at 0.1 and $\alpha$ takes on values 0.5, 0.78, and 0.84. It may be noted that we observed contours with negative curvature for the Romero–Vanden-Broeck branches of finger solutions for the sufficiently large surface tension parameter $\kappa$ (in the McLean–Saffman notation). However, we could not find any bubble shape whose front agrees with these finger shapes in the same way as the main branch solutions agree with the McLean–Saffman branch of finger solutions for $\alpha$ approaching 1. It is possible that there are bubble solutions that tend to the Romero–Vanden-Broeck branch of solutions but do not continue to $\epsilon = 0.1$ and $\alpha = 0.5$ in the parameter space and were therefore inaccessible to our search procedure. A more exhaustive search is needed to find other branches if they exist. For the extraordinary branch of bubble solutions, we were unable to calculate accurate solutions for bigger values of $\epsilon$ and $\alpha$ than the ones reported in Table II. The method outlined is not suitable for such calculations because these bubbles have large curvatures at unpredictable points on the bubble contour. It is also not clear whether the extraordinary branch of solution exists beyond a very limited region in the parameter space. We have to substantially modify our numerical procedure to answer these questions as well as the question of whether it is possible to have bubbles that elongate indefinitely in the positive $x$ direction as $\epsilon$ tends to infinity. If that

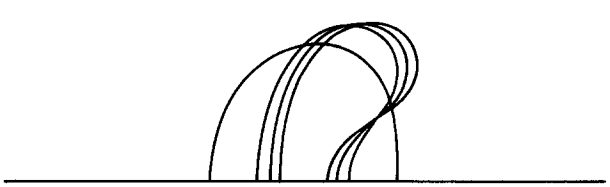

FIG. 6. The shapes of an extraordinary bubble for $\alpha = 0.5$ and $\epsilon = 0.15$, 0.2, 0.22, and 0.24. The bubbles which are more deformed correspond to larger values of $\epsilon$.

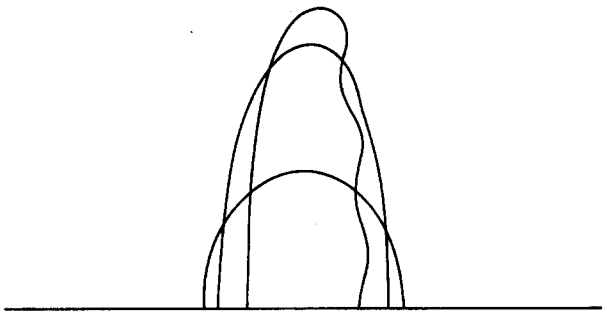

FIG. 7. The shape of extraordinary bubbles for $\epsilon = 0.1$ and $\alpha = 0.5$, 0.78, and 0.84. The more vertically elongated bubbles correspond to larger values of $\alpha$.

is not the case, the circle remains the only possible contour shape for a bubble in the limit of infinite $\epsilon$.

## X. DISCUSSIONS AND CONCLUSION

We have calculated the effect of surface tension on a Hele–Shaw cell bubble. The degeneracy of the Taylor–Saffman solutions is removed by the effect of surface tension. We analyzed the perturbation scheme for small surface tension in detail and arrive at the conclusion that even though a regular perturbation series is consistent, it does not account for exponential order terms that are singular in the flow domain, which occur unless the bubble velocity takes on specific isolated value or values for given area and surface tension. The occurrence of exponentially small terms in this perturbation problem is surprising because the regular perturbation series is found to be consistent to all orders and one would not suspect the occurrence of exponential terms. This may serve as a cautionary tale in the widespread application of perturbation techniques.

Further, we find that bubble solutions are not unique. We find a second solution over some range in the parameter space. The detailed features of this have not been thoroughly investigated. However, the existence of other bubble solutions, which in the limit of infinite elongation agrees with Romero–Vanden-Broeck branches of finger solutions, remains an open question. We were, however, unable to find these. Further investigation in this direction is left for the future; so is the study of the effect of variation of transverse curvature. For the case of a finger, the variation of transverse curvature has a substantial effect as has been recently demonstrated by Reinelt and Saffman.[11] The study of the stability of these bubble solutions is important and will also be a topic for future investigation.


## ACKNOWLEDGMENTS

This problem was suggested to me by Professor P. G. Saffman. I wish to thank him for all his interest, encouragement, and several illuminating discussions and comments. I also benefited from discussions with Professor M. Klaus, Dr. W. Henshaw, and Michael Ward. The math department Vax 11/780 at VPI and the fluid dynamics Vax 11/750 in the Department of Applied Math at Caltech were used for numerical calculations and permission for their generous use is very much appreciated.

This work was supported by the Department of Energy, Office of Basic Energy Sciences Grants DEAS05-80ER-10711 and DEAT03-76ER-72012 and the Exxon Educational Foundation.

[1]P. G. Saffman and G. I. Taylor, Proc. Soc. London Ser. A **245**, 312 (1958).
[2]T. Maxworthy, submitted to J. Fluid Mech.
[3]G. I. Taylor and P. G. Saffman, Q. J. Mech. Appl. Math. **12**, 265 (1959).
[4]J. W. McLean and P. G. Saffman, J. Fluid Mech. **102**, 455 (1980).
[5]L. Romero, Ph.D. dissertation, Dept. of Applied Math California Institute of Technology, Pasadena, 1982.
[6]J. M. Vanden-Broeck, Phys. Fluids **26**, 2033 (1983).
[7]B. I. Shraiman, submitted to Phys. Rev.
[8]R. Combescot, T. Dombre, V. Hakim, Y. Pomeau, and A. Pumir, submitted to Phys. Rev. Lett.
[9]D. C. Hong and J. S. Langer, submitted to Phys. Rev. Lett.
[10]L. Kandanoff (private communication with P. G. Saffman).
[11]D. A. Reinelt and P. G. Saffman, Siam J. Sci. Stat. Comput. **6**, 542 (1985).